

Small-angle neutron scattering measurements of the vortex lattice in CaC_6

R. Cubitt,¹ J. S. White,¹ M. Laver,¹ M. R. Eskildsen,² C. D. Dewhurst,¹ D. McK. Paul,³ A. J. Crichton,³ M. Ellerby,⁴ C. Howard,⁴ Z. Kurban,⁴ and F. Norris⁴

¹*Institut Laue Langevin, 6 Jules Horowitz, 38042 Grenoble, France*

²*Department of Physics, University of Notre Dame, Notre Dame, Indiana 46556, USA*

³*Department of Physics, University of Warwick, Coventry CV4 7AL, United Kingdom*

⁴*Department of Physics and Astronomy, University College London, Gower Street, London WC1E 6BT, United Kingdom*

(Received 8 January 2007; revised manuscript received 30 March 2007; published 27 April 2007)

Small-angle neutron scattering has been applied to study the vortex lattice in the intercalated graphite superconductor CaC_6 ($T_c = 11.3$ K). Scattering from the vortex lattice is in the form of a ring, most likely reflecting the absence of in-plane orientational order of the pyrolytic graphene planes. The temperature and field dependence of the scattered intensity allows the in-plane zero temperature value of the coherence length [$\xi = 350(25)$ Å] and the London penetration depth [$\lambda = 500(30)$ Å] to be estimated. Measurements with the applied field at 70° to the c axis directly reveal the penetration depth anisotropy, $\gamma_\lambda = 5.1(4)$, which, unlike MgB_2 , is equal to the anisotropy of the coherence length deduced from magnetization measurements. The orientation of the vortex lattice is fixed relative to the rotation axis of the crystal as predicted by anisotropic London theory.

DOI: [10.1103/PhysRevB.75.140516](https://doi.org/10.1103/PhysRevB.75.140516)

PACS number(s): 74.70.Ad, 71.20.Tx, 74.25.Qt

The intercalation of graphite with metallic atoms has long been known to produce superconducting compounds.¹ However, interest has been renewed with the recent discovery of superconductivity in CaC_6 exhibiting a remarkably high $T_c \approx 11.3$ K,² almost an order of magnitude higher than the previously known intercalated graphites. A conventional BCS, phonon mediated mechanism behind the superconductivity is strongly suggested by the presence of an isotope effect,³ the absence of gap nodes deduced from heat capacity,⁴ a single gap from spectroscopy measurements⁵ and a conventional temperature dependence of the London penetration depth, λ .⁶ The presence of two bands contributing to the superconductivity in MgB_2 , a similarly structured material, was evidenced by the inequality between the penetration depth anisotropy, γ_λ , and that of the coherence length, γ_ξ .⁷ It is notoriously difficult to measure λ derived from magnetization measurements of the lower critical field, B_{c1} , as pinning and surface barrier effects tend to mask the point of departure from the purely diamagnetic Meissner state. Neutron scattering allows us to directly measure the penetration depth and its anisotropy in an unambiguous manner by probing the vortex lattice (VL) spacing in different directions when the applied field is at a large angle to the c axis. The field dependence of the integrated intensity of the scattering provides us with a direct measurement of λ and ξ via the modified London form factor. These values are consistent with an analysis modeling the temperature dependence of the form factor close to T_c with GL theory.

The VL in type II superconductors results in a spatially oscillating magnetic field in the plane perpendicular to the magnetic field direction. The amplitude of this modulation is determined by the two characteristic length scales λ and ξ . For a given internal field, shorter λ results in a lower minimum field between vortices, whilst shorter ξ gives a higher peak field in the normal core of a vortex. The neutron, with its associated magnetic moment, can scatter from planes of vortices, producing a pattern of Bragg peaks related to the symmetry of the real space vortex arrangement. Experiments

were carried out on the small-angle neutron scattering (SANS) beamline D22 at the Institut Laue-Langevin using neutrons of wavelength 16.5 Å with 10% wavelength spread. Two single crystals made up the sample used in these experiments, both cleaved from the same crystal and prepared under the same conditions as described previously.⁸ The two crystals had masses of 4.06(2) and 2.90(1) mg and identical T_c 's of 11.3(2) K. The sample was cooled through T_c in an applied field, almost parallel to the neutron beam, to form a VL. In this manner, the sample need only be rocked by small angles to illuminate the various Bragg peaks and to measure the total scattered or “integrated” intensity of a particular Bragg reflection. A measurement of the background nuclear scattering was subtracted from all low temperature data to leave only the signal from the VL. Magnetization measurements were made using a vibrating sample magnetometer to determine the upper critical field, $B_{c2}(T)$, as function of temperature.

Figure 1 shows $B_{c2}(T)$ for fields applied parallel and perpendicular to the crystal c axis. The solid line in Fig. 1 is a fit using an approximation to BCS theory⁹ and extrapolates to a $T_c(0) = 11.3(2)$ K for both field directions. The two upper critical fields extrapolated to zero temperature are $B_{c2}(0) \perp = 0.99(1)$ T and $H_{c2}(0) \parallel = 0.214(3)$ T. The ratio of the critical fields, $\gamma_\xi = B_{c2\perp}/B_{c2\parallel} = \xi_{\parallel}/\xi_{\perp} = 4.6(1)$ is a measure of the ratio of the coherence lengths parallel and perpendicular to the c axis. A similar value $\gamma_\xi = 5$ has been derived from the resistive transition.¹⁰ In this paper we report these values are comparable to the ratio of the corresponding London penetration depths, $\gamma_\lambda = 5.1(1)$.

Figure 2 shows the diffraction image from the vortex lattice following field cooling in 50 and 80 mT to 2 K. The observed ring of scattered intensity shows that the VL is disordered, or at least polycrystalline with many differently oriented domains of VL. This is not surprising since it is well known that the ab planes in pyrolytic graphite do not have very long-range orientational order and that the VL tends to

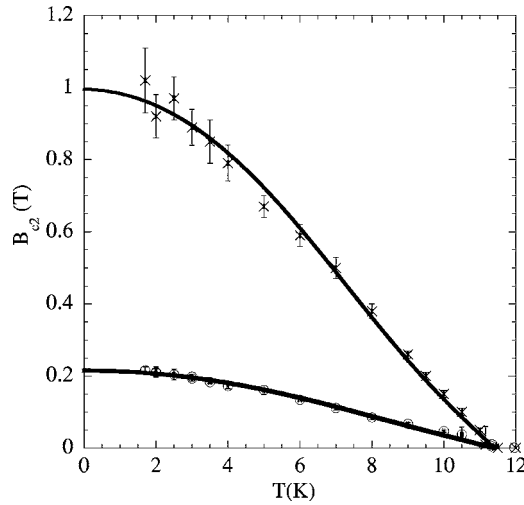


FIG. 1. $B_{c2}(T)$ derived from superconducting quantum interference device (SQUID) magnetization measurements. The upper data are with $B \parallel ab$ and the lower with $B \parallel c$. The fits are empirical approximations to BCS theory yielding $B_{c2}(0) \parallel c = 0.214(3)$ T and $B_{c2}(0) \parallel ab = 0.99(1)$ T. $T_c(0) = 11.3(1)$ K.

align itself¹¹ to a specific crystalline direction. Nevertheless, we find that a precise measurement of the scattering vector, q , of the Bragg ring is consistent with interplane vortex spacing of hexagonal VL domains. Consequently, we have for the integrated intensity summed the neutron counts within a 60° sector of the Bragg ring, which for any given VL domain will contain the scattering from exactly one Bragg peak. The rocking curve at 50 mT, shown in the inset to Fig. 3, has a remarkably wide full-width-half-maximum (FWHM) of $14(2)^\circ$ corresponding to a VL longitudinal correlation length of $\sim 0.8 \mu\text{m}$. The rocking curve width provides a measure of the longitudinal correlation length of vortices; this may be diminished due to a finite sample size as in powders or pinning-induced disorder.

The integrated intensity of the rocking curve, I , is related

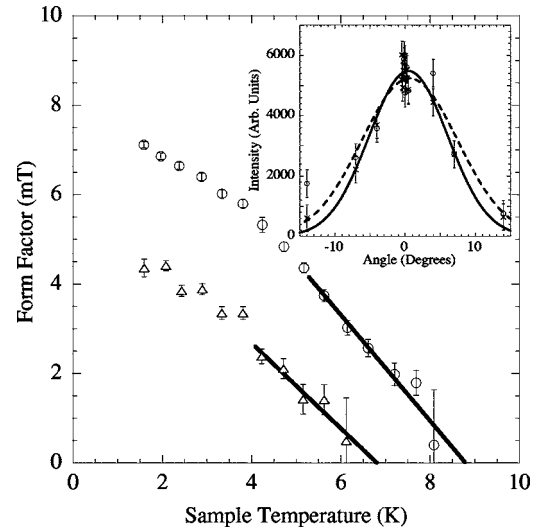


FIG. 3. The temperature dependence of the form factor from 1.5 K to T_c , in applied fields of 50 mT (circles) and 80 mT (triangles). The solid lines are high- T linear fits used to determine dF/dT . The inset shows the wide rocking curves taken at 2 K as described in the text, with the solid curves representing the left side of the ring and the dashed curve the right side. The cluster of points about the zero degrees angle confirms the absence of any feature superposed on top of the broader rocking curve.

to the Fourier component of the spatial variation of the magnetic field, or form factor F by the relation:¹²

$$I = 2\pi V \phi \left(\frac{\gamma}{4} \right)^2 \left(\frac{\lambda_n^2}{\Phi_0^2 q} \right) |F|^2. \quad (1)$$

Here, V is the illuminated sample volume, ϕ is the incident neutron flux density, γ is the neutron magnetic moment in nuclear magnetons, λ_n is the neutron wavelength, Φ_0 is the flux quantum, and q is the magnitude of the scattering vector. The London form factor, F (applicable for $\kappa = \infty$) can be

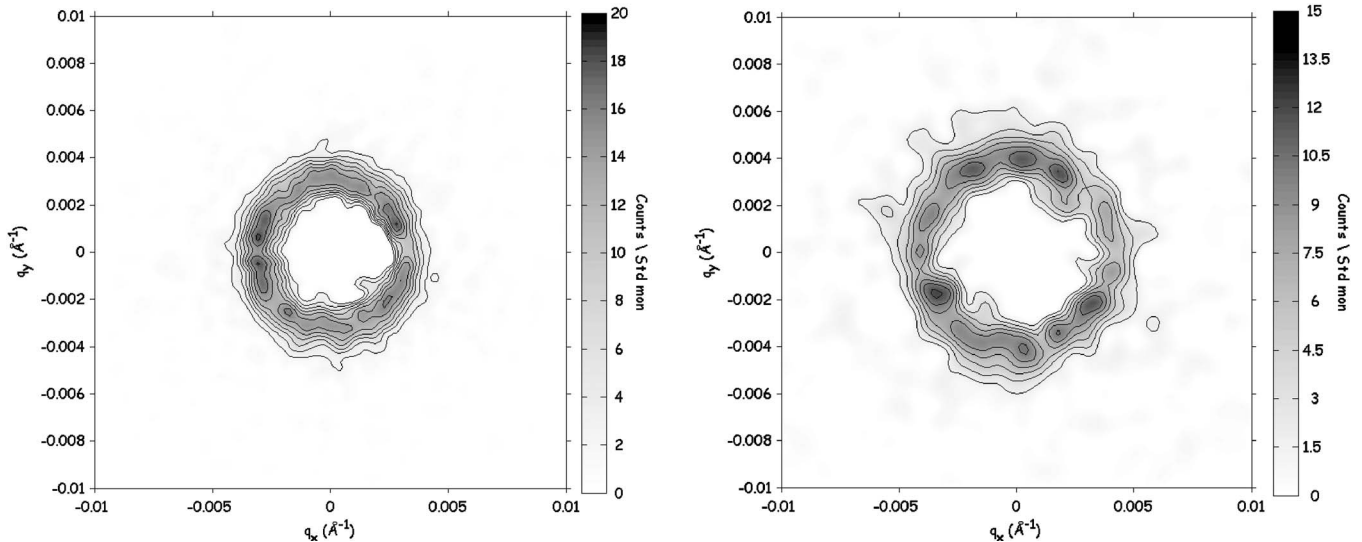


FIG. 2. The intensity ring in counts/standard beam monitor due to neutron scattering from the flux lattice with $H \parallel c$ in an applied field of 50 mT (left) and 80 mT (right). Data has been smoothed and noise from the very central region masked.

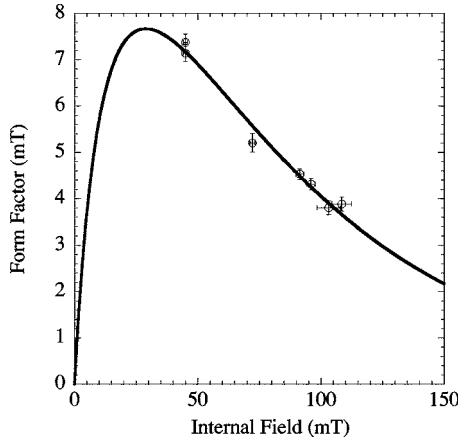


FIG. 4. Measured form factor as a function of B at 2 K, with the internal field derived from the measured q vector. The fit is the modified London equation (2) with $C=0.5$, yielding values $\lambda_{ab}=500(20)$ Å and $\xi_{ab}=350(35)$ Å.

modified by an exponential term to account for the finite size of the vortex cores as

$$F = \frac{Be^{-C\xi^2q^2}}{1 + (\lambda q)^2}, \quad (2)$$

where B is the average internal field, λ is the penetration depth, ξ is the coherence length, and C is a constant with a value between 0.25 and 2.¹³ Figure 3 shows the temperature dependence of F for applied fields of 50 and 80 mT. For temperatures approaching T_c , F decreases linearly with temperature as expected from Ginsburg-Landau (GL) theory.¹⁴ Knowing the gradient dF/dT near T_c and the gradient of dB_{c2}/dT from Fig. 1 and using the approach of Forgan *et al.*,¹⁵ we can deduce two almost identical values for $\kappa = \lambda_{ab}/\xi_{ab}$ at the two temperature ranges considered: $\kappa(50 \text{ mT}, 5-9 \text{ K}) = 1.17(7)$ and $\kappa(80 \text{ mT}, 4-7 \text{ K}) = 1.18(7)$.

Taking $\xi_{ab}(0)$ to be $392(3)$ Å from $B_{c2}\parallel c(T=0)$ gives a value for $\lambda_{ab}(0) = 459(35)$ Å, making the reasonable assumption that κ at $T=0$ is the same as that found over the two temperature ranges. The exponential correction term in (2) is essentially empirical and has not been verified for low κ materials, and would certainly not be applicable close to B_{c2} where $F \rightarrow 0$. Using a value of $C=0.5$ ^{7,13} we can make a fit of the data at low temperatures yielding values of $\lambda_{ab} = 500(30)$ Å and $\xi_{ab} = 350(20)$ Å, as shown in Fig. 4 and in good agreement with the values derived above.

Applying the London formula, $n = m_e/\lambda^2\mu_0e^2$, assuming no electronic mass enhancement, and using $\lambda_{ab}(0) = 500(30)$ Å, we can derive the number density of superconducting electrons, n at $T=0$ to be $1.1(1) \times 10^{22} \text{ cm}^{-3}$. This corresponds to 0.10(1) superconducting electrons per carbon atom using the known lattice parameters.¹⁶ Using n and the normal state resistivity ($\rho = 1 \mu\Omega \text{ cm}$ Ref. 17) we can estimate the dirtiness of the superconductivity, L/ξ_{ab} where the mean free path, $L = v_F m_e / (\rho n e^2)$ and $\xi_{ab} = \hbar v_F / (1.764 k T_c)$ giving $L/\xi_{ab} = 2.5(3)$ placing the material just in the clean limit.

To obtain γ_λ , the sample was rotated so that the applied field was at an angle of 70° with respect to the c axis. The anisotropy of the penetration depth induces a distortion of the vortex lattice so that the Bragg peaks no longer lie on a circle but on an ellipse, with an aspect ratio directly related to the penetration depth anisotropy.^{7,11} Campbell *et al.*¹⁸ predict a specific orientation of the vortex lattice with respect to the ellipse axes, i.e. that Bragg peaks should lie on the minor axis. The elliptical distortion and this preferential orientation are shown in Fig. 5 at 80 mT. The increased intensity on the vertical axis is not simply due to the difference in the magnitude of the scattering vectors in the horizontal and vertical directions. Taking into account the different value of q_y and comparing the $B\parallel c$ and $B\angle 70^\circ$ measurements there is an increase in intensity in the q_y direction in the 70° case showing that intensity has moved from other directions round the

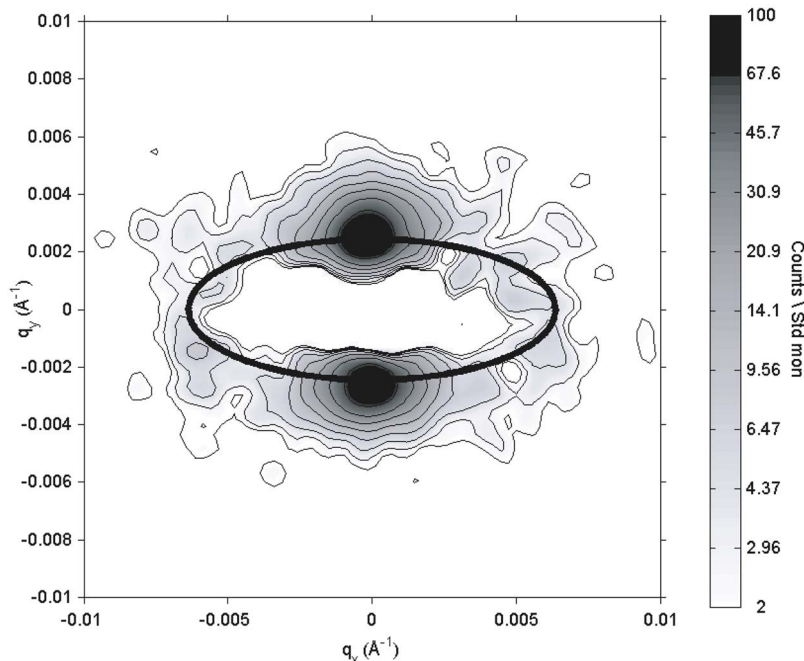


FIG. 5. The diffracted neutron intensity in counts/standard beam monitor with an applied field of 80 mT at an angle of 70° to the c axis. The overlaid ellipse has an aspect ratio calculated from fitting the intensity along the vertical and horizontal axes. Data has been smoothed and noise from the very central region masked.

ellipse into the q_y direction due to an orientational effect. Finally, the intense peak in the q_y direction is not simply due to an absence of intensity in other directions, as this is ~ 5 times larger than that expected if there were no orientational effect. The high intensity diffraction spots observed in the minor axis directions, q_y are thus a satisfying confirmation of the prediction of Campbell *et al.*. The low intensity in the major axis direction, q_x where four other spots are expected, is most likely due to disorder induced by vortices crossing defects in the ab plane. Using Campbell's approach, γ_λ is found directly from the ratio of major to minor axes of the ellipse ε , by

$$\gamma_\lambda^2 = \varepsilon^2 \left(\frac{\sin^2 \psi}{1 - \varepsilon^2 \cos^2 \psi} \right), \quad (3)$$

where $\psi = 70^\circ$ is the angle between the applied field and the c axis. The axes ratio of the ellipse in Fig. 5 was obtained from integrating the intensity over 7° sectors along the ellipse axes. The resulting values were $|q_x| = 0.00632(9) \text{ \AA}^{-1}$ and $|q_y| = 0.00246(3) \text{ \AA}^{-1}$ giving the axis ratio, $\varepsilon = 2.57(5)$. Using (3) we obtain $\gamma_\lambda = 5.1(4)$ which agrees well with γ_ξ derived from the data in Fig. 1. Due to the layered nature of CaC_6 , it is natural to consider a comparison between this compound and MgB_2 . Our current study made two measurements of the anisotropy to search for evidence of double band/gap

behavior.⁷ The agreement between the two anisotropy parameters, γ_ξ and γ_λ , is consistent with the single band nature of the superconductivity but does not rule out the unlikely possibility of multiple bands with identical anisotropies. It is of interest to note that the anisotropy found in the Yb compound, which has a very similar c axis lattice parameter, is only ~ 2 as deduced from measurements of the critical fields.²

In conclusion, there is remarkable agreement between the value of κ deduced from the modified London form factor (2) and that found from dF/dT with a GL approach. The values of λ_{ab} found are somewhat lower than the only value published, to our knowledge, of $720(80) \text{ \AA}$,⁶ measured using mutual inductance techniques. The unusually large rocking curve width of 14° corresponds to a short correlation length of the vortex lattice along the field direction of 0.8 \mu m . A possible explanation is this length corresponds to the average grain size along the c axis of crystallites of aligned carbon planes. If the vortex lattice is pinned orientationally to a crystal direction in the carbon planes, the result would be a ring of scattering corresponding to all orientations of the crystallites consistent with these observations. The extra intensity in the minor axis direction of the ellipse of scattering found when the applied field was 70° to the c axis confirms the prediction from anisotropic London theory.¹⁸

¹N. B. Hannay, T. H. Geballe, B. T. Matthias, K. Andres, P. Schmidt, and D. MacNair, *Phys. Rev. Lett.* **14**, 225 (1965).

²T. E. Weller, M. Ellerby, A. S. Saxena, R. P. Smith, and N. T. Skipper, *Nat. Phys.* **1**, 39 (2005).

³D. G. Hinks, D. Rosenmann, H. Claus, M. S. Bailey, and J. D. Jorgensen, *Phys. Rev. B* **75**, 14509 (2007).

⁴J. S. Kim, R. K. Kremer, L. Boeri, and F. S. Razavi, *cond-mat/0603539* (unpublished).

⁵N. Bergeal, V. Dubost, Y. Noat, W. Sacks, D. Roditchev, N. Emery, C. Hérol, J. F. Mareche, P. Lagrange, and G. Loupías, *Phys. Rev. Lett.* **97**, 077003 (2006).

⁶G. Lamura, M. Aurino, G. Cifariello, E. DiGennaro, A. Andreone, N. Emery, C. Hérol, J.-F. Marêché, and P. Lagrange, *Phys. Rev. Lett.* **96**, 107008 (2006).

⁷R. Cubitt, M. R. Eskildsen, C. D. Dewhurst, J. Jun, S. M. Kazakov, and J. Karpinski, *Phys. Rev. Lett.* **91**, 047002 (2003).

⁸S. Pruvost, C. Hérol, A. Hérol, and P. Lagrange, *Carbon* **42**, 1825 (2004).

⁹T. P. Sheahen, *Phys. Rev.* **149**, 368 (1966).

¹⁰E. Jobiliong, H. D. Zhou, J. A. Janik, Y. J. Jo, L. Balicas, J. S.

Brooks, and C. R. Wiebe, *cond-mat/0604062* (unpublished).

¹¹P. L. Gammel, D. A. Huse, R. N. Kleiman, B. Batlogg, C. S. Oglesby, E. Bucher, D. J. Bishop, T. E. Mason, and K. Mortensen, *Phys. Rev. Lett.* **72**, 278 (1994).

¹²D. K. Christen, F. Tasset, S. Spooner, and H. A. Mook, *Phys. Rev. B* **15**, 4506 (1977).

¹³A. Yaouanc, P. Dalmas de Réotier, and E. H. Brandt, *Phys. Rev. B* **55**, 11107 (1997).

¹⁴V. L. Ginzburg and L. D. Landau, *Zh. Eksp. Teor. Fiz.* **20**, 1064 (1950).

¹⁵E. M. Forgan, S. J. Levett, P. G. Kealey, R. Cubitt, C. D. Dewhurst, and D. Fort, *Phys. Rev. Lett.* **88**, 167003 (2002).

¹⁶N. Emery, C. Hérol, M. d'Astuto, V. Garcia, Ch. Bellin, J. F. Marêché, P. Lagrange, and G. Loupías, *Phys. Rev. Lett.* **95**, 087003 (2005).

¹⁷A. Gauzzi, S. Takashima, N. Takeshita, C. Terakura, H. Takagi, N. Emery, C. Hérol, P. Lagrange, and G. Loupías, *cond-mat/0603443* (unpublished).

¹⁸L. J. Campbell, M. M. Doria, and V. G. Kogan, *Phys. Rev. B* **38**, 2439 (1988).